Korean J. Chem. Eng., 37(10), 1660-1668 (2020)
DOI: 10.1007/s11814-020-0553-y

pISSN: 0256-1115
eISSN: 1975-7220

Effects of cellulose, hemicellulose and lignin on biomass pyrolysis kinetics

Lingli Zhu and Zhaoping Zhong†

Key Laboratory of Energy Thermal Conversion and Control of Ministry of Education, School of Energy and Environment, Southeast University, Nanjing 210096, P. R. China
(*Received 7 December 2019 • Revised 1 April 2020 • Accepted 4 April 2020*)

Abstract−In order to investigate interactions among biomass components on pyrolysis kinetics, pyrolysis experiments of individual components, synthetic biomass (designed by Design-Export software) and natural biomass (rice husk and corn straw) were conducted on a thermogravimetric analyzer (TGA). The results revealed that the pyrolysis behavior of cellulose is sharp, which is with low pyrolysis reaction order (1.38), high activation energy (168.61 kJ/mol) and high pre-exponential factor (3.50E+12 /s). The pyrolysis behavior of hemicellulose and lignin is slower but more complicated, both with high pyrolysis reaction order (2.30, 1.51), low activation energy (126.31, 87.21 kJ/mol), and low pre-exponential factor (9.67E+09, 2.59E+05 /s). Comparison of the experimental and calculated kinetics of synthetic samples confirmed that interactive effects on pyrolysis kinetics exist in the co-pyrolysis process. In particular, the presence of lignin inhibited the pyrolysis reaction rate of synthetic biomass, and cellulose played the dominant role in the activation energy and frequency factor. The pyrolysis reaction order was strongly influenced by hemicellulose owing to its abundant and complex branched chains. The predicted model was also established for calculating kinetic parameters of natural biomass with known proportions of three components. The predicted results were consistent with the experimental ones, validating the effectiveness of the prediction model.

Keywords: Biomass Components, Pyrolysis, Kinetics, Interactive Effects, Prediction

INTRODUCTION

Biomass energy has received extensive attention due to its potential as an alternative, renewable and environment-friendly energy source [1]. To date, thermochemical conversion technology. including combustion, liquefaction and gasification, has been the primary application of biomass energy. Pyrolysis, as the primary step for the thermochemical conversion of biomass materials, has been extensively studied in recent decades [2]. Research on pyrolysis kinetics of biomass can help reveal the reaction mechanism of thermochemical utilization process, predict the reaction rate and difficulty and provide an important basis for development of biomass thermochemical conversion.

Biomass is a complex polymer with a chemical composition that includes cellulose, hemicellulose, lignin and some extractives. Cellulose, as the largest component of biomass, is a straight chain polymer linked by glycosidic bonds. Intermolecular and intermolecular hydrogen bonds in cellulose are interacted by three hydroxyl groups in each glucose monomer, resulting in a stable crystal structure and unique mechanical strength. Hemicellulose, as a polysaccharide polymer with abundant branched chains, consists of xylose, arabinose, mannose and glucose. Hemicellulose has a degree of polymerization (DP) of 50-200 monomers, much lower than cellulose. Hemicellulose exhibits poor stability due to its amorphous structure. Among them, lignin with the most complicated structure, is a random three-dimensional network polymer which is difficult to decompose by reason of connected phenylpropane units. Natural biomass pyrolysis is considered as a comprehensive performance of the co-pyrolysis of cellulose, hemicellulose and lignin.

The interaction among three biomass components during co-pyrolysis process is commonly evaluated by their pyrolysis behavior and product characteristics. Pang et al. predicted natural biomass pyrolysis profiles in the assumption of the pyrolysis behavior of three biomass components were mutually independent during co-pyrolysis process, and the predicted results were with some degree of accuracy [3]. Yang et al. studied the thermogravimetric characteristics of three biomass components on a TGA [4]. The pyrolysis results of synthesized biomass samples indicated that the interaction among three biomass components were trivial. On the contrary, some other researchers declared that the pyrolysis behavior of natural or synthesized biomass cannot be deemed the simple superposition of cellulose, hemicellulose, lignin accounting for their obvious interactions. Liu et al. observed the existence of interactions among three major biomass components during co-pyrolysis on a thermogravimetric analyzer coupled with Fourier transform infrared spectrometer (TG-FTIR) [5]. The TG curves revealed that significant interaction occurred below 327 °C, above 327 °C for lignin to hemicellulose, hemicellulose to cellulose, respectively. The FTIR spectra results showed that lignin inhibited the formation of 2-furaldehyde and C=O containing substances, while the presence of hemicellulose caused the strong inhibition of the formation of levoglucosan and promotion of the formation of hydroxyl acetaldehyde. Zhao et al. obtained the same conclusion by the experiments of synthetic biomass by a pyrolysis-gas chromatography/mass spectroscopy (Py-GC/MS) [6]. Yu et al. investigated different reactivities among three biomass components pyrolysis in a TG and a

†To whom correspondence should be addressed.
E-mail: zzhong@seu.edu.cn

Table 1. The proximate, ultimate and componential analyses of samples

Samples	Proximate analysis, *ad* (%)				Ultimate analysis, *daf* (%)					Componential analysis (%)		
	Moisture	Volatile	Ash	Fixed carbon	C	H	O	N	S	Cellulose	Hemicellulose	Lignin
C	6.6	88.8	0.2	4.4	44.0	6.0	49.5	0.4	0.1	100.0	0.0	0.0
H	6.5	76.2	5.0	12.3	40.3	5.8	53.5	0.3	0.1	0.0	100.0	0.0
L	6.9	67.1	2.9	23.1	58.2	5.5	35.4	0.8	0.1	0.0	0.0	100.0
RH	7.3	62.5	17.7	12.5	35.6	7.2	56.7	0.4	0.1	45.4	30.3	24.3
CS	8.1	70.3	11.2	10.4	39.2	8.1	52.4	0.2	0.1	49.3	31.8	18.9

C: cellulose, H: hemicellulose, L: lignin, RH: rice husk, CS: corn straw, ad: air dried basis; daf: dry ash free basis.

wire mesh reactor [7]. It indicated that the experimental results of pyrolysis products were in good agreement with predicted results based on the behavior of biomass individual components, suggesting the lack of interaction at low pyrolysis temperature (below 325 °C). However, interactions were significant between cellulose and hemicellulose, lignin at higher pyrolysis temperatures (above 325 °C). These interactions caused the decrease of tar yields, increase of char yields and change of tar products distribution.

To understand in-depth the pyrolysis mechanism of biomass, acknowledgment of the kinetics parameters is prerequisite [8]. Song et al. calculated the kinetic parameters of biomass pyrolysis by using different analytic methods [9], and showed that there was no significant impact of different methods on kinetics values. Reverte et al. found that optimizing the experiment design was beneficial to evaluate the kinetics model based on various experimental schemes [10]. Most researches employed TGA, Py-GC/MS or fixed beds to investigate the pyrolysis behavior of biomass. The interactions among three biomass components can be analyzed qualitatively, and there was still a slight divergence in the interaction between hemicellulose and lignin co-pyrolysis. The aim of this work was to establish valid mathematical models for predicting kinetic parameters of natural biomass based on the proportion of three major components and explore the influence of interactions on pyrolysis kinetics quantitatively. To date, the investigations on the interactive effects among three major biomass components are still lacking and in disagreement. This work explored the correlation between chemical compositions of biomass, including cellulose, hemicelluloses and lignin, and kinetic rates of biomass pyrolysis. It also offers a new sight to predict the kinetic characteristics of biomass pyrolysis and provide a deeper theoretical basis for the utilization of biomass energy.

MATERIALS AND METHOD

1. Materials

Microcrystalline cellulose, xylan from beech wood and alkali lignin (Sigma-Aldrich) were chosen to represent the three major biomass components. Rice husk from the rural area of Anhui province in China was used to evaluate the prediction model of pyrolysis kinetic parameters. These samples were crushed into powder and the average particle size of cellulose, hemicellulose, lignin and rice husk was about 50, 100, 50 and 100 μm, respectively. All samples were dried at 105 °C in the oven for 10 h to eliminate external moisture.

2. Characteristic Analysis

The proximate analysis was determined by the National Standard of China (GB/T 212-2008) which was based on the dry ash free basis. The ultimate analysis of samples was determined by Vario Micro cube (Elementar) and based on the air-dried basis. The content of fixed carbon and O was obtained by differential subtraction. The componential analysis of the crude biomass (rice husk, corn straw) was determined by Van's component analysis method [11]. The proximate, ultimate and componential analyses of three biomass components and natural biomass are shown in Table 1.

3. Experimental Methods

The mixed samples were designed on the point of a grid according to the Simplex-lattice mixture design method. The mass fractions of cellulose, hemicellulose and lignin were defined as X_C, X_H and X_L, which in natural biomass was about 30-65, 10-50 and 10-50%, respectively [12]. It indicated a specially constrained design, where $0.30 \le X_C \le 0.65$, $0.10 \le X_H \le 0.50$, $0.10 \le X_L \le 0.50$ and $X_C + X_H + X_L = 1$. Design-Expert software was employed for the specific design. A total of 12 experimental points are shown in Fig. 1, where three points are individual biomass components, three points are binary synthetic biomass and six points are ternary synthetic biomass [8,13].

4. Thermogravimetric Analysis

The pyrolysis characteristics of all biomass samples were evaluated on a thermogravimetric analyzer. Al_2O_3 was as the material of crucible. Nitrogen with high purity (>99.999%) was chosen as the carrier gas, which flow rate was 120 ml min^{-1}. About 10 mg of the sample was heated from 25 to 800 °C under a constant heating rate of 10 °C min^{-1}. Each experiment was repeated at least three times

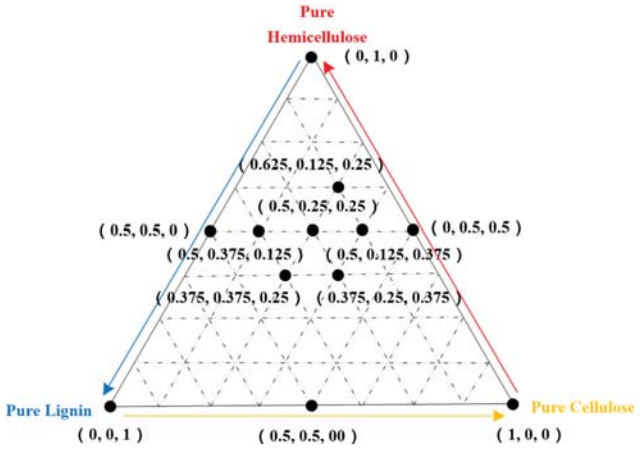

Fig. 1. The mixture design scheme by Design-Expert software (the values in parentheses correspond to X_C, X_H, X_L, respectively).

to ensure the accuracy of the statistical experiment. The weight loss rate (dW/dt) and conversion proportion (α) of the sample are as follows:

$$\alpha = \frac{W_0 - W_t}{W_0 - W_f} \quad (1)$$

$$\frac{d\alpha}{dt} = -\frac{1}{W_0 - W_f}\left(\frac{dW_t}{dt}\right) \quad (2)$$

where, W_0 is the initial mass of sample, W_t is the sample mass when the pyrolysis time is t min. W_f is the mass at the terminal pyrolysis time, mg.

5. Kinetic Model

The TGA curves show the overall thermogravimetric characteristics of biomass. According to the Arrhenius law, the kinetic Eq. (3) of biomass pyrolysis in the non-isothermal process can be shown as follows [14]:

$$\frac{d\alpha}{dt} = K(1-\alpha)^n = A\exp\left(-\frac{E}{RT}\right)(1-\alpha)^n \quad (3)$$

where, A represents the frequency factor, E represents the activation energy, T is the absolute temperature, R is the gas constant, and n is the reaction order. In addition, the constant heating rate, β, is shown as the following, Eq. (4):

$$\beta = \frac{dT}{dt} \quad (4)$$

Eq. (5) is derived from Eqs. (1) and (3), offering a different description of the kinetic law:

$$\frac{d\alpha}{dT} = \frac{A}{\beta}\exp\left(-\frac{E}{RT}\right)(1-\alpha)^n \quad (5)$$

The activation energy and frequency factor can be obtained by the Coats-Redfern integral method as shown in the following, Eqs. (4) and (5) [15-18]:

With the 1_{st} order of reaction,

$$-\ln\left[\frac{-\ln(1-\alpha)}{T^2}\right] = -\ln\left[\frac{AR}{\beta E}\left(1-\frac{2RT}{E}\right)\right] + \frac{E}{RT} \quad (6)$$

With the n_{th} order of reaction,

$$-\ln\left[\frac{-\ln(1-\alpha)^{(1-n)}}{T^2(1-n)}\right] = -\ln\left[\frac{AR}{\beta E}\left(1-\frac{2RT}{E}\right)\right] + \frac{E}{RT} \quad (7)$$

where, $\frac{2RT}{E} \ll 1$ and $-\ln\left[\frac{AR}{\beta E}\left(1-\frac{2RT}{E}\right)\right]$ is almost a constant, E and A are calculated by the slope and intercept of first-order fitting curve by drawing $-\ln\left[\frac{-\ln(1-\alpha)}{T^2}\right]$ (n=1) or $-\ln\left[\frac{-\ln(1-\alpha)^{(1-n)}}{T^2(1-n)}\right]$ (n≠1) vs. $\frac{1}{T}$.

RESULTS AND DISCUSSION

1. Pyrolysis of Biomass Individual Component

The curves of thermal mass loss rate (α) and differential thermal gravity (DTG) of individual biomass component (cellulose, hemicellulose and lignin) are presented in Fig. 2. The pyrolysis process of biomass components can be divided into three stages: the initial stage of dehydration, the second stage of degradation, and the final stage of decarbonization. Cellulose was gradually transited into active cellulose, and curves presented as a platform in the initial stage [19]. The characteristic parameters of the pyrolysis of individual biomass components are listed in Table 2; the pyrolysis progress of cellulose was sharp in a narrow temperature range (240-350 °C), which represented typical characteristics of linear polymers [20]. The total mass loss rate value of cellulose pyrolysis was 94.7%. There were double peaks in the DTG curve of hemicellulose owing to its two distinct structural units. The initial temperature of hemicellulose's devolatilization was low (200 °C) compared to that of cellulose (240 °C) due to more branched chains and poor thermal stability of hemicellulose [21]. For the complicated structure, lignin had been losing weight slowly during the pyrolysis progress [22]. The pyrolysis rate was the lowest one among the three components and tended to produce more coke (47.9%). The activity criterion was defined based on the TG curves and pyrolysis characteristics. The temperature point A of DTG curve where the phenomenon of dehydration occurred was called the critical point. High activity point was

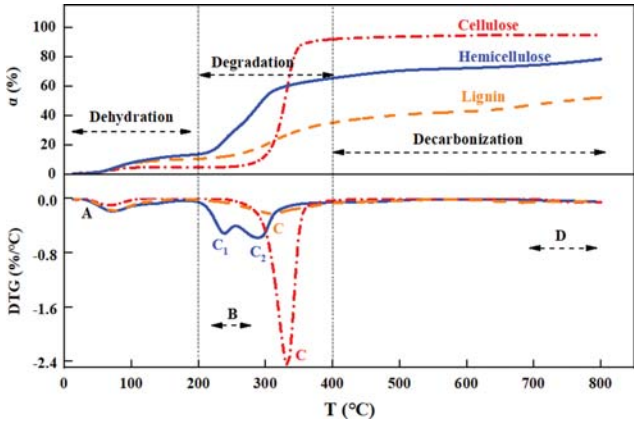

Fig. 2. The α and DTG curves of individual biomass component.

Table 2. Characteristic parameters of single biomass components during pyrolysis

Samples	Stage	Temperature range	Mass loss rate	Total mass loss rate
		T (°C)	α_n (%)	α (%)
C	I	25-240	4.7	94.7
	II	240-350	81.9	
	III	350-800	8.1	
H	I	25-200	13.4	78.3
	II	200-400	51.9	
	III	400-800	13.0	
L	I	25-240	11.9	52.1
	II	240-500	28.3	
	III	500-800	11.9	

Table 3. Relevant parameters for activity criterion of single biomass components

Samples	Relevant parameters				
	Critical point	High activity point	Low activity point		Stagnation point
	A (°C)	B (°C)	C_1 (°C)	C_2 (°C)	D (°C)
C	34	240-270	332	-	700-800
H	26	200-220	238	302	700-800
L	31	240-280	310	-	700-800

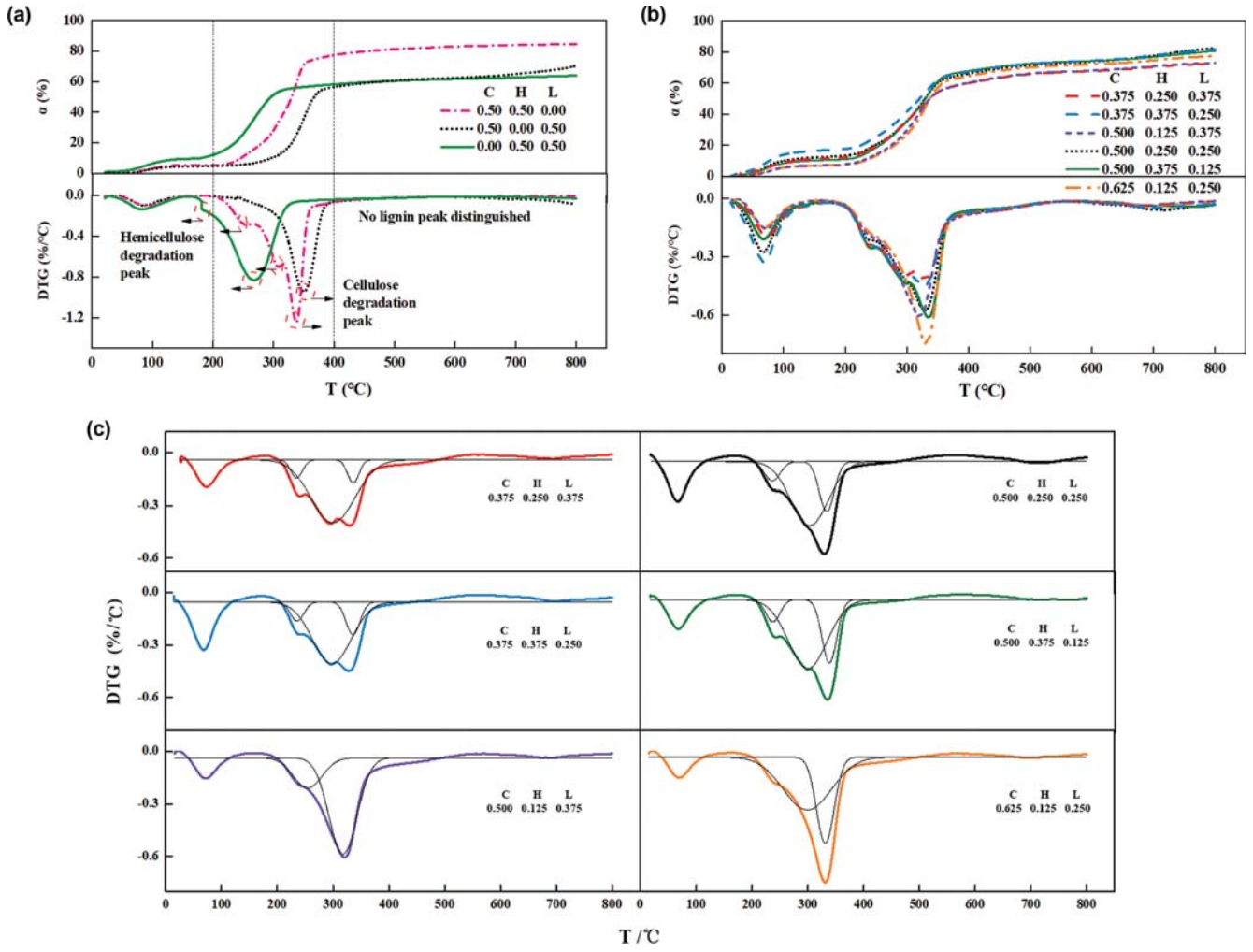

Fig. 3. The comparison of α, DTG curves of the binary synthetic biomass (a), ternary synthetic biomass (b) and deconvoluted curves of ternary synthetic biomass (c).

defined as the temperature point B where the mass loss rate was rapidly increased. Before reaching the temperature point C (low activity point), the pyrolysis rate gradually slowed. Until the temperature point D (stagnation point), the pyrolysis behavior of biomass was almost negligible. The high activity point of hemicellulose was 200-220 °C, which was lower than that of other two components. In addition, there were two low activity points in the TG curve of hemicellulose pyrolysis. These results were consistent with poor thermal stability and structural composition of hemicellulose. The details of relevant parameters of three biomass components based on activity criterion are shown in Table 3.

2. Pyrolysis of Synthetic Samples

The α and DTG curves of biomass binary mixture during co-pyrolysis process are shown in Fig. 3(a). The DTG curve of cellulose and hemicellulose co-pyrolysis shows three obvious degradation peaks at 250, 305, 330 °C. The first two peaks were dominated by the hemicellulose decomposition, and the other was caused by the cellulose decomposition. It seemed that there was no obvious synergistic effect on the co-pyrolysis of cellulose and lignin due to the similar degradation temperatures of their individual pyrolysis. In terms of the co-pyrolysis of cellulose and lignin, there was a single degradation peak at 360 °C on the DTG curve. Compared to

Table 4. Comparison of activation energy for cellulose, hemicellulose, and lignin in the recent studies with literature values

Component	Temperature range	Frequency factor	Reaction order	Activation energy	Correlation coefficient	Literature value	References
	T (°C)	A (1/s)	N	E (kJ/mol)	X	E (kJ/mol)	
Cellulose	200-400	3.50E+12	1.38	168.61	0.9951	134.50, 223.32, 178.48, 200.00, 164.30, 154.00	[8,24-28]
Hemicellulose	200-400	9.67E+09	2.30	126.31	0.9775	114.8, 73.85, 144.41, 85.00, 116.73	[13,24,25,29,30]
Lignin	200-400	2.59E+05	1.51	87.19	0.9824	107.6, 23.41, 74.91, 52.00, 69.43	[13,24,25.31,32]

the individual pyrolysis, the pyrolysis temperature of cellulose shifted to the higher temperature and its mass loss rate was significantly decreased. These phenomena reflected that cellulose degradation was inhibited in the presence of lignin. The DTG curve of hemicellulose and lignin co-pyrolysis exhibited a weak shoulder at 180 °C and an obvious peak at 270 °C. The two degradation peaks of hemicellulose overlapped in the presence of lignin, which was also observed by Wang et al. [23]. It could be inferred that the two structural units of hemicellulose were affected by lignin during the co-pyrolysis process. The α, DTG and deconvoluted curves of biomass ternary mixtures during the co-pyrolysis process are shown in Fig. 3(b) and (c). The temperatures where degradation peaks occurred on the DTG curve were determined by the mixing proportions of cellulose and hemicellulose. The second degradation peak became weaker with decreasing proportion of hemicellulose, which was overlapped by the degradation peak of cellulose. In addition, the maximum mass loss rate was positively correlated with the cellulose proportion. With the increasing proportion of lignin, the primary pyrolysis interval of synthetic biomass tended to move to the higher temperature side. In general, cellulose and hemicellulose play a major role in the release of volatiles, while lignin has a negative effect on thermal mass loss rate of synthetic biomass samples.

3. Pyrolysis Kinetics Analysis

The mass loss rate of biomass component pyrolysis in the initial and terminal stages was slow and unstable, causing large measurement errors. It had an adverse effect on the accuracy of kinetic parameter calculation. The kinetic calculation of this work excluded the stages of dehydration and decarbonization. The selected temperature for the fitting calculation ranged from 200 to 400 °C. The detailed kinetic parameters including frequency factor (A), reaction order (N), activation energy (E), correlation coefficient (X) of biomass samples during the primary pyrolysis process are listed in Table 4. Among the pyrolysis of three biomass components, cellulose had the minimum value of reaction order (1.38), the maximum value of activation energy (168.61 kJ/mol) and frequency factor (3.50E+12 /s). It revealed its simple structure unit, strong thermal stability and rapid pyrolysis reaction. The most correlation coefficients obtained by data fitting were above 0.9, but that of hemicellulose pyrolysis data was relevantly low due to its instability. Furthermore, the pyrolysis reaction of hemicellulose tended to deviate from the first reaction order, which indicated its complex pyrolysis mechanism caused by plenty of branched chains. The lowest values of activation energy (87.19 kJ/mol) and frequency factor (2.59E+05 /s) showed the low pyrolysis reaction rate of lignin. Table 4 shows the comparison of the activation energies obtained using Coats-Redfern integral method (primary degradation stage: 200-400 °C), with values from previous studies. It indicates that kinetic method is more reliable and accurate in predicting the activation

Table 5. Comparison of experimental and calculated kinetic parameters of biomass pyrolysis

Sample code	Temperature range	Frequency factor		Reaction order		Activation energy		Correlation coefficient	
	T (°C)	A (1/s)		N		E (kJ/mol)		X	
		Exp.	Cal.	Exp.	Cal.	Exp.	Cal.	Exp.	Cal.
(0.500, 0.500, 0.000)	200-400	2.38E+08	1.75E+12	1.55	1.84	118.34	147.46	0.9814	0.9863
(0.500, 0.000, 0.500)	200-400	2.02E+06	1.75E+12	0.93	1.45	102.73	127.91	0.9866	0.9888
(0.000, 0.500, 0.500)	200-400	9.48E+02	4.83E+09	1.25	1.91	89.03	106.76	0.9757	0.9800
(0.375, 0.250, 0.375)	200-400	6.84E+06	1.17E+12	1.73	1.73	99.41	127.38	0.9778	0.9850
(0.375, 0.375, 0.250)	200-400	3.98E+06	1.56E+12	1.66	1.72	97.11	136.42	0.9791	0.9864
(0.500, 0.125, 0.375)	200-400	3.04E+06	1.94E+12	1.58	1.53	96.86	136.78	0.9835	0.9889
(0.500, 0.250, 0.250)	200-400	2.06E+06	1.95E+12	1.55	1.61	95.10	141.12	0.9800	0.9884
(0.500, 0.375, 0.125)	200-400	6.62E+06	1.95E+12	1.57	1.70	100.34	145.47	0.9784	0.9878
(0.625, 0.125, 0.250)	200-400	2.09E+06	2.33E+12	1.44	1.51	96.43	145.82	0.9753	0.9903

energy of the pyrolysis of biomass.

It was assumed that the three components of biomass were independent of each other during the co-pyrolysis process. The calculated pyrolysis kinetics (A, N, E and X) of synthetic biomass could be obtained by weighted average method. The experimental and calculated kinetic parameters of synthetic biomass (200-400 °C) are shown in Table 5. Compared to the calculated values, the experimental frequency factor values were lower. It was deduced that the pyrolysis reaction rates of mixed samples were decreased significantly, which might be the reason for the inhibition of lignin to the decomposition of cellulose and hemicellulose. There was a slight difference between the experimental and calculated values of reaction order. It demonstrated that the complexity of pyrolysis mechanism was not affected much by interactions among biomass components. Furthermore, the lower experimental values of activation energy suggested that the initiate pyrolysis temperatures of synthetic biomass moved forward under the influence of hemicellulose component. It may be owing to its abundant and complex branched chain structure. The influence on correlation coefficient could be ignored due to the similar values. The comparison of experimental and calculated kinetic parameters confirmed that the co-pyrolysis behavior of the synthetic biomass samples should not be regarded as the simple superposition of the individual components. The existence of significant interactions among three biomass components could be effectively certified by the change rule of kinetics parameters. To improve the accuracy of pyrolysis kinetics prediction of natural biomass, the influence of interaction among three biomass major components on kinetics quantificationally is required

Table 6. The analysis of variance (ANOVA) for regression models

Source	Sum of squares	Degree of freedom	Mean square	F value	p-Value
(a) Activation energy E					
Model	10131.32	9	1125.70	9375.27	<0.0001
Linear mixture	5023.68	2	2511.84	20919.54	<0.0001
X_CX_H	1132.57	1	1132.57	9432.47	<0.0001
X_CX_L	510.59	1	510.59	4252.36	<0.0001
X_HX_L	252.81	1	252.81	2105.46	<0.0001
$X_CX_HX_L$	17.46	1	17.46	145.44	<0.0001
X_CX_H (X_C-X_H)	10.39	1	10.39	86.50	<0.0001
X_CX_L (X_C-X_L)	17.83	1	17.83	148.53	<0.0001
X_HX_L (X_H-X_L)	4.67	1	4.67	38.92	0.0004
Residual	0.84	7	0.12		
Total	10132.16	16			
(b) Frequency factor A					
Model	2.155E+025	9	2.394E+024	592.97	<0.0001
Linear mixture	1.007E+025	2	5.034E+024	1246.58	<0.0001
X_CX_H	4.097E+024	1	4.097E+024	1014.63	<0.0001
X_CX_L	2.442E+024	1	2.442E+024	604.81	<0.0001
X_HX_L	1.142E+020	1	1.142E+020	0.028	0.8712
$X_CX_HX_L$	1.778E+023	1	1.778E+023	44.04	0.0003
X_CX_H (X_C-X_H)	1.347E+022	1	1.347E+022	3.34	0.1105
X_CX_L (X_C-X_L)	1.411E+022	1	1.411E+022	3.50	0.1037
X_HX_L (X_H-X_L)	1.980E+021	1	1.980E+021	0.49	0.5064
Residual	2.827E+022	7	4.038E+021		
Total	2.158E+025	16			
(c) Reaction order N					
Model	1.71	9	0.19	78.76	<0.0001
Linear mixture	1.09	2	0.54	224.53	<0.0001
X_CX_H	0.11	1	0.11	44.20	0.0003
X_CX_L	0.20	1	0.20	82.97	<0.0001
X_HX_L	0.35	1	0.35	143.10	<0.0001
$X_CX_HX_L$	0.44	1	0.44	180.55	<0.0001
X_CX_H (X_C-X_H)	3.246E-004	1	3.246E-004	0.13	0.7250
X_CX_L (X_C-X_L)	7.540E-004	1	7.540E-004	0.31	0.5940
X_HX_L (X_H-X_L)	0.017	1	0.017	7.16	0.0317
Residual	0.017	7	2.419E-003		
Total	1.73	16			

to taken into account.

4. Prediction and Verification

4-1. Prediction Model

The biomass pyrolysis experiments were designed by Design-Expert mixing method and the prediction model was proposed to investigate the pyrolysis kinetics of natural based on the proportion of three biomass major components. There were 12 pyrolysis experiments points of biomass components mixtures including single component, binary mixture and ternary mixture. The experimental pyrolysis kinetics (A, N, E and X) was obtained by Coats-Redfern method. The proportion of three biomass components was considered as independent variables (X_C, X_H and X_L), and kinetic parameters represented the response values (Y) in the fitting modeling analysis of prediction model. The regression equation was as follows:

$$Y=A_CX_C+A_HX_H+A_LX_L+A_{CH}X_CX_H+A_{CL}X_CX_L+A_{HL}X_{HL}+A_{CHL}X_{CHL} \quad (8)$$

where, $0.30\le X_C\le 0.65$, $0.10\le X_H\le 0.50$, $0.10\le X_H\le 0.50$ and $X_C+X_H+X_L=1$. A_C, A_H, A_L, A_{CH}, A_{CL}, A_{HL} and A_{CHL} are the linear and nonlinear coefficients. The regression equations of kinetic parameters (A, N, E and X) could be obtained by experimental data of 12 pyrolysis experiments points. The results were as follows:

$$\begin{aligned}A=&3.49E+12X_C+9.68E+09X_H-1.82E+08X_L\\&-7.00E+12X_CX_H-7.39E+12X_CX_H\,(X_C-X_H)\\&-6.93E+12X_CX_L-7.17E+12X_CX_L\,(X_C-X_L)\\&-4.78E+10X_HX_L+4.57E+12X_HX_L\,(X_H-X_L)\\&+1.12E+13X_CX_HX_L\end{aligned} \quad (9)$$

$$\begin{aligned}N=&1.38X_C+2.30X_H+1.51X_L\\&-1.13X_CX_H-1.15X_CX_H\,(X_C-X_H)\\&-1.99X_CX_L+1.66X_CX_L\,(X_C-X_L)\\&-2.63X_HX_L-13.51X_HX_L\,(X_H-X_L)\\&+17.62X_CX_HX_L\end{aligned} \quad (10)$$

$$\begin{aligned}E=&168.59X_C+126.31X_H+87.21X_L\\&-116.32X_CX_H-205.11X_CX_H\,(X_C-X_H)\\&-100.27X_CX_L-254.92X_CX_L\,(X_C-X_L)\\&-71.05X_HX_L-221.98X_HX_L\,(X_H-X_L)\\&+111.41X_CX_HX_L\end{aligned} \quad (11)$$

$$\begin{aligned}X=&0.99X_C+0.98X_H+0.98X_L\\&-0.019X_CX_H-0.064X_CB\,(X_C-X_H)\\&-6.478E\text{-}03X_CX_L-0.062X_CX_L\,(X_C-X_L)\\&-0.018X_HX_L-0.024X_HX_L\,(X_H-X_L)\\&-0.035X_CX_HX_L\end{aligned} \quad (12)$$

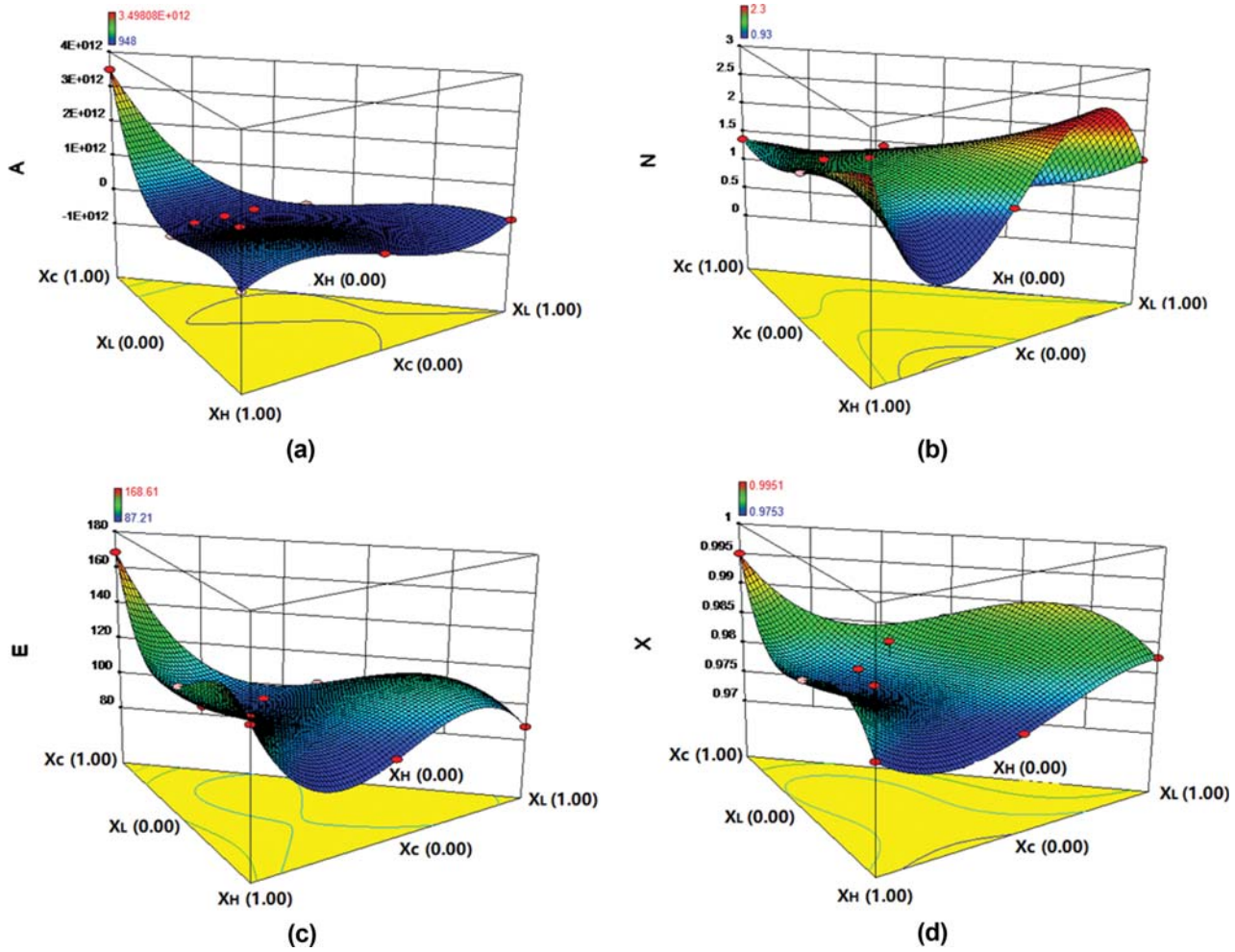

Fig. 4. The 3D response surfaces for the predicted kinetic values including A, N, E and X.

The analysis of variance (ANOVA) on regression models of key parameters was performed to confirm the interaction effect. As listed in Table 6, the p-value of each model was less than 0.0001, which revealed that these regression models had good fitting significance. The determination coefficient R^2 of each model was above 0.99, indicating that the models fitted well. Hence, these models were valid to predict pyrolysis kinetic parameters of biomass with known proportions of three components.

The 3D response surfaces based on the regression equations were employed to explore the influence of interactions among three biomass components on kinetic parameters. The lengths between each point on the response surface and the three-coordinate plane represented the mass fractions of cellulose, hemicellulose, and lignin (the sum of the lengths was 1). The strength of interaction among three biomass components on kinetic parameters was associated with the shape and gradient of response surfaces. The shape of the curve face indicated that interaction of influence factors occurred while the plane was the opposite. The greater gradient of the curved surface indicated that the influence of the interaction between factors on the response value was stronger. Thus, the three factors (cellulose, hemicellulose and lignin) interacted with each other according to a non-linear changing trend. The shape of plane demonstrated that the gradient was invariable, which indicated that response values had a good linear relationship with the influence factors. As shown in Fig. 4(a)-(d), three biomass components had an interactive effect on the pyrolysis kinetic parameters of biomass, and the biomass pyrolysis process was not a simple superposition of the three-component pyrolysis processes. The pyrolysis of cellulose had little influence on the reaction order, while hemicellulose and lignin had a greater influence on the reaction order. With the increasing proportion of hemicellulose and lignin components, the influence of hemicellulose and lignin on the reaction order was enhanced. The pyrolysis of cellulose played a dominant role in the values of activation energy and pre-exponential during the co-pyrolysis of biomass three-component mixture. Compared with cellulose, hemicellulose and lignin had little influence on those. Moreover, the correlation coefficient was synthetically affected by cellulose, hemicellulose and lignin.

4-2. Verification and Comparison

It can be obtained by the deformation of Eqs. (6) and (7) based on the Coats-Redfern integral method:

For the 1_{st} order of reaction,

$$\alpha=1-\exp\left(-\frac{ART^2}{\beta E}\left(1-\frac{2RT}{E}\right)\exp\left(-\frac{E}{RT}\right)\right) \quad (13)$$

For the n_{th} order of reaction,

$$\alpha=1-\left(1-(n-1)\left(-\frac{ART^2}{\beta E}\right)\left(1-\frac{2RT}{E}\right)\exp\left(-\frac{E}{RT}\right)\right)^{\frac{1}{1-n}} \quad (14)$$

The componential analysis of natural biomass (rice husk and corn straw) is shown in Table 1. Their corresponding kinetic parameters were calculated by Eqs. (9)-(12) of the prediction model, and then the pyrolysis weight loss curve was obtained by Eq. (13) or (14). The comparison on TG curves of natural biomass and predicted model is presented in Fig. 5, and the correlation coefficients

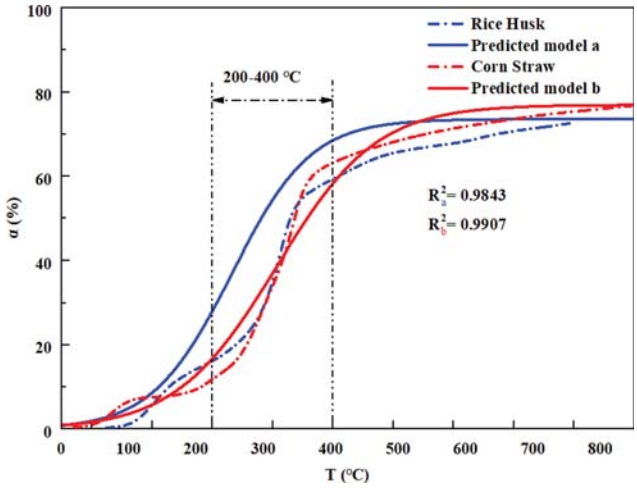

Fig. 5. The TG curves of natural biomass and predicted model.

R^2 of TG curves are calculated and analyzed. The results showed that the correlation coefficient R_a^2 between the two TG curves of rice husk and predicted model was 0.9843, while that for corn straw and predicted model (R_b^2) was 0.9907. It indicated that the TG curves of prediction model were reasonable, and values obtained by the prediction model agreed well with the experimental data of natural biomass. The pyrolysis of natural biomass tended to produce more solid residues in the end. Raveendran et al. carried out acid pickling pretreatment on 13 kinds of biomass before pyrolysis experiments [19]. They found that the initial pyrolysis temperature moved up and maximum pyrolysis rate of biomass after ash removal increased. It was known that natural biomass was composed of a small amount of extractives and inorganics, which was almost nondecomposable. Besides, the inorganics had an apparent catalytic effect on the pyrolysis process of biomass, which might be the reason for lower initial pyrolysis temperature of natural biomass [33-35]. In short, this model could effectively predict the kinetic parameters of biomass pyrolysis based on the proportions of the three components. Note that the pyrolysis behavior was determined by not only three major biomass components, but also a small amount of extractives and inorganics. The existence of extractives and inorganics promoted the yield of char and had a significant effect on the pyrolysis reaction rate [36].

CONCLUSIONS

The pyrolysis behavior of cellulose was sharp and fast, with pyrolysis reaction order of 1.38, activation energy of 168.61 kJ/mol and frequency factor of 3.50E+12 /s. The pyrolysis behavior of hemicellulose and lignin was slower but more complicated, which were both with higher pyrolysis reaction order (2.30, 1.51), lower activation energy (126.31, 87.21 kJ/mol), and lower frequency factor (9.67E+09, 2.59E+05 /s).

The interactive effects among three biomass components on pyrolysis kinetics were confirmed by the comparison of experimental and calculated kinetics of synthetic biomass. In particular, cellulose played a dominant role on activation energy and frequency factor owing to its single structure unit and rapid pyrolysis charac-

teristic. The pyrolysis reaction order was strongly influenced by hemicellulose and lignin.

Compared to the TG curves of synthetic biomass and the predicted model, the initial pyrolysis temperature of natural biomass increased. It might be the reason for the catalytic effect of minerals in natural biomass on pyrolysis reaction. The kinetic parameters obtained by the prediction model were relatively reasonable and accurate, and values obtained by the prediction model agreed well with the experimental data of natural biomass. In short, this model could effectively predict the kinetic parameters of biomass pyrolysis based on their proportions of three components.

ACKNOWLEDGEMENTS

This work was financially supported by the National Natural Science Foundation of China (grant nos. 51776042).

REFERENCES

1. E. D. Gordillo and A. Belghit, *Fuel Process. Technol.*, **92**, 314 (2011).
2. E. Ranzi, A. Cuoci and T. Faravelli, *Energy Fuel*, **22**, 4292 (2008).
3. C. H. Pang, S. Gaddipatti, G. Tucker and E. Lester, *Bioresour. Technol.*, **172**, 312 (2014).
4. H. P. Yang, R. Yan and H. P. Chen, *Energy Fuel*, **20**, 388 (2011).
5. Q. Liu, Z. Zhong and S. Wang, *J. Anal. Appl. Pyrol.*, **90**, 213 (2011).
6. S. Zhao, M. Liu and L. Zhao, *Ind. Eng. Chem. Res.*, **57**, 5241 (2018).
7. J. Yu, N. Paterson and J. Blamey, *Fuel*, **191**, 140 (2017).
8. Y. Fan, J. Xia and L. Jiao, *Energy Convers. Manage.*, **138**, 106 (2017).
9. C. C. Song, H. Q. Hu and S. W. Zhu, *J. Fuel Chem. Technol.*, **31**, 311 (2003).
10. R. Cédric, J. L. Dirion and M. Cabassud, *J. Anal. Appl. Pyrol.*, **79**, 297 (2007).
11. T. Hosoya, H. Kawamoto and S. Saka, *J. Anal. Appl. Pyrol.*, **80**, 118 (2007).
12. S. Wang, X. Guo and K. Wang, *J. Anal. Appl. Pyrol.*, **91**, 183 (2011).
13. P. Thanatawee, W. Rukthong and S. Sunphorka, *Int. J. Chem. React. Eng.*, **14**, 517 (2016).
14. T. Damartzis, D. Vamvuka, S. Sfakiotakis and A. Zabaniotou, *Bioresour. Technol.*, **102**, 6230 (2011).
15. H. Song, *Acta Energiae. Solaris. Sinica*, **29**, 716 (2008).
16. R. Gottipati and S. Mishra, *J. Fuel Chem. Technol.*, **39**, 265 (2011).
17. P. B. Gangavati and M. J. Safi, *Thermochim. Acta*, **428**, 63 (2005).
18. S. Xing, H. Yuan and Huhetaoli, *Energy*, **114**, 634 (2016).
19. Q. Liu, S. Wang and K. Wang, *Acta Phys.-Chim. Sinica*, **24**, 1957 (2008).
20. S. Wang, Z. Xia and Q. Wang, *J. Anal. Appl. Pyrol.*, **126**, 118 (2017).
21. S. Wang, B. Ru and H. Lin, *Bioresour. Technol.*, **143**, 378 (2013).
22. Q. Liu, S. Wang and K. Wang, *Korean J. Chem. Eng.*, **26**, 548 (2009).
23. S. Wang, X. Guo and K. Wang, *J. Anal. Appl. Pyrol.*, **91**, 183 (2011).
24. W. Cao, J. Li, M. Teresa and X. Zhang, *J. Energy Inst.*, **92**, 1303 (2019).
25. J. Yeo, B. Chin, J. Tan and Y. J. Loh, *J. Energy Inst.*, **92**, 27 (2019).
26. V. Mamleev, S. Bourbigot and J. Yvon, *J. Anal. Appl. Pyrol.*, **80**, 151 (2007).
27. G. Özsin, *Bioresour. Technol.*, **300**, 122700 (2020).
28. L. P. Luo, X. J. Guo, Z. Zhang and M. J. Chai, *Energy Fuel*, **34**, 4874 (2020).
29. R. Moriana, Y. Zhang, P. Mischnick and J. Li, *Carbohydr. Polym.*, **106**, 60 (2014).
30. Y. M. Ding, B. Q. Huang, K. Y. Li and W. Z. Du, *Energy*, **195**, 117010 (2020).
31. D. Karla, D. Stephen and F. D. Rory, *Combust. Inst.*, **37**, 2697 (2019).
32. K. R. G. Burra and K. Gupta, in AIAA Scitech 2020 Forum, AIAA (2020).
33. K. Raveendran, A. Ganesh and K. C. Khilar, *Fuel*, **74**, 1812 (1995).
34. S. L Zhao, M. Liu and L. Zhao, *Korean J. Chem. Eng.*, **34**, 1 (2017).
35. H. P. Yang, H. P. Chen and D. U. Sheng-Lei, *Proceed. Csee.*, **29**, 70 (2009).
36. S. L. Zhao, M. Liu and L. Zhao, *Korean J. Chem. Eng.*, **34**, 3077 (2017).